SCIENCE CHINA
Technological Sciences

•Article•

December 2023 Vol.66 No.12: 3504–3521
https://doi.org/10.1007/s11431-023-2459-8

Energy-optimized adaptive cruise control strategy design at intersection for electric vehicles based on speed planning

PAN ChaoFeng[1], LI Yuan[1*], HUANG AiBao[1], WANG Jian[2] & LIANG Jun[1]

[1] *Automotive Engineering Research Institute, Jiangsu University, Zhenjiang 212013, China;*
[2] *School of Automotive and Traffic Engineering, Jiangsu University, Zhenjiang 212013, China*

Received January 27, 2023; accepted July 3, 2023; published online October 10, 2023

In this study, vehicle queuing was investigated at intersections to propose an eco-driving strategy to improve vehicle energy consumption and traffic efficiency in urban traffic environments. The proposed design approach can be applied to electric vehicles, and the control framework is categorized into two layers. In the upper layer, the speed of the host vehicle is planned offline, and in the lower layer, the required control variable acceleration is determined. First, the energy optimization problem of electric vehicles passing through an intersection was constructed, and the planning vehicle speed was obtained based on the genetic algorithm (GA). Next, the speed tracking controller and distance tracking controller were designed using sliding mode control (SMC) to ensure that the vehicle can track the planning speed with safe vehicle spacing. Finally, combined with specific cases, the energy-saving effect of the proposed method in the single-vehicle scenario, and the presence of manual driving vehicles in front- and multi-vehicle driving scenarios were studied. The results revealed that the GA-based single-vehicle speed planning method reduced energy consumption by up to 16% compared with the rule-based speed planning method. Furthermore, compared with the intelligent driver model (IDM) and adaptive cruise control (ACC) methods, the GA fleet speed planning method based on V2X communication can reduce average fleet energy consumption by 26% and 24%, respectively, and improve intersection traffic efficiency. The results of the sensitivity analysis of factors affecting planned speed revealed that vehicles passing through intersections at a steady speed exhibited superior economic performance. Finally, hardware-in-the-loop (HIL) testing was performed to verify the effectiveness of the controller under real-time conditions.

electric vehicle, intersections, eco-driving, speed planning, V2X, sliding mode control

Citation: Pan C F, Li Y, Huang A B, et al. Energy-optimized adaptive cruise control strategy design at intersection for electric vehicles based on speed planning. Sci China Tech Sci, 2023, 66: 3504–3521, https://doi.org/10.1007/s11431-023-2459-8

1 Introduction

With the severity of environmental pollution and resource shortages increasing, green travel is becoming crucial [1]. Electric vehicles are an effective method to reduce carbon emissions and oil dependency. However, electric vehicles exhibit the problems of range anxiety. Therefore, saving energy and increasing the range of electric vehicles has become a critical topic of discussion. In this regard, energy-optimal adaptive cruise control (EACC) systems are an effective solution [2,3] and considerably improve safety [4], comfort [5] and economy [6]. The rapid development of advanced driver assistance systems and autonomous driving can further improve EACC [7,8].

In recent years, numerous studies have focused on scenarios such as motorways [9], hillsides [10], urban roads [11], and intersections [12], to determine the energy-saving potential for each scenario and increase the public acceptance of EACC. In the application scenario, the EACC under the intersection is highly complex. Most existing EACC studies integrate vehicle driving energy consumption into the ACC controller by introducing the economic evaluation

*Corresponding author (email: 2222104121@stmail.ujs.edu.cn)

index [13] and formulating a multi-objective optimization problem with constraints based on the weight coefficients to obtain the optimal control variables such as acceleration, motor, or engine torque [14]. The design of EACC at the intersection includes the optimization of integer variables such as traffic behavior decision of crossing the intersection currently as well as nonlinear factors such as motor energy consumption. If the problem is transformed into a multi-objective optimization problem, the problem may involve considerable calculation. Moreover, complex nonlinear optimization algorithms are also required [15].

According to the various objects, intersection research can be classified into two types [16]. In one method, more vehicles are allowed to pass by optimizing traffic signal timing. In the other method, parking and idling times are reduced by optimizing the speed sequence of vehicles in the queue. Most existing methods for optimizing traffic signal timing are based on the premise that traffic signal timing can be adjusted. In a previous study [14], datasets collected by conventional fixed traffic sensors were used to predict future traffic conditions. A traffic light dynamic optimization strategy (DTSTOS) based on various vehicle fuel consumption and dynamic characteristics was used to minimize total energy consumption and traffic delay [17]. In ref. [18], traffic light strategies based on fixed-time, adaptive-time, and reinforcement learning algorithms were compared experimentally. The results revealed that system performance improved considerably after using the RMART information-sharing algorithm. However, applying this system in practice is difficult because of the complexity of traffic systems.

The optimization of the speed sequence of the vehicle does not require changing the traffic signal timing. This method is effective in various intersection scenarios. Studies have revealed that speed planning can reduce the vehicle idling time and the number of stops, which reduces energy consumption. In existing studies, speed planning at intersections can be categorized into rule-based and optimization-based methods. In the rule-based speed optimization algorithm, the planned speed is obtained according to the laws of physics to ensure intersection passing without stopping. Specifically, planning reduces the overall vehicle energy consumption by reducing motor idling and travel time. In ref. [11], a rule-based uniform speed movement strategy was proposed to use the remaining time of the signal light and the distance from the intersection to plan the speed, which avoids vehicles stopping at the green light. In ref. [19], a dynamic speed planning algorithm was proposed to maximize the probability that the traffic light is green when a vehicle approaches an intersection. Although the rule-based approach improves energy consumption, the uniform speed movement planning strategy reduces speed planning flexibility and does not optimize the speed from the perspective of motor energy consumption. Unlike rule-based strategies, optimization-based speed planning methods are highly flexible and consider numerous constraints when solving the cost function to obtain an optimized vehicle speed sequence. In ref. [20], the Pontryagins's minimum principle was used to optimize the speed sequence of connected vehicles, which improves traffic flow. A multi-stage dynamic planning method was proposed [21] to optimize vehicle speeds around signalized intersections by adding additional variables such as the road gradient and weather conditions, which achieved positive results.

However, most intersection studies focused on the speed planning and control of the host vehicle and ignore the interaction between the host and surrounding vehicles. For example, in ref. [22], the fuel saving problem of a single vehicle passing through multiple signal intersections was investigated. In this study, a realistic vehicle system dynamics model was used to improve fuel economy. In ref. [23], a multi-objective hierarchical optimization strategy was proposed for hybrid electric vehicle speed planning and energy management, which reduces the probability of stopping at intersections through speed planning of the host vehicle. An adaptive speed planning method for connected autonomous vehicles based on multi-light training deep reinforcement learning was proposed [24]. In ref. [25], V2I and V2V technologies were used to develop a novel method for speed control through continuous signal intersections in a connected environment. In this method, connected information was used to optimize vehicle speed. These studies revealed that speed planning for a single vehicle can effectively reduce vehicle fuel consumption and emissions. However, although the host vehicle can pass the intersection at an economical speed and obey traffic rules, the vehicle may affect the driving status of surrounding vehicles. For example, when the average planning speed of the controlled vehicle is too low, the efficiency of intersection traffic can decrease considerably. Although the interaction of environmental vehicles has been investigated, a study [26] proposed a novel reinforcement learning method based on ES-DQN. An intelligent speed control strategy was proposed for uncertain cut-in scenarios. This result revealed a superior adaptability and control effect than the conventional ACC control strategy. To solve the problem of multimodal driving intention in surrounding vehicles, a multimodal driving intention partially observable Markov decision process (MDI-POMDP) decision framework [27] was developed to realize safe and effective behavior decision-making and movement planning. To improve the performance of vehicle motion planning, a novel BRAM-ED trajectory prediction framework was proposed [28] to improve prediction accuracy and provide a basis for motion planning in complex scenarios. However, most studies have focused on safety performance and are yet to consider traffic efficiency and economy. Furthermore, intersection speed planning studies are based on conventional fuel vehicles or hybrid electric vehicles.

However, in the future, electric powertrains will be developed, which may result in distinct eco-driving behaviors because of the distinct characteristics of the powertrain and control objectives.

Therefore, in order to solve the problem above, this paper proposes an intersection EACC design method for electric vehicles based on hierarchy structure design. The upper layer is used to plan the speed of the host vehicle offline, and the lower layer is used to determine the required control variable acceleration, allowing the main vehicle to better track the planned speed and ensure driving safety. At the same time, in order to improve the robustness of the controller, this paper designs the lower layer controller based on sliding mode control (SMC) theory and linear matrix inequality (LMI) theory. The speed tracking controller is used to track the desired speed, and the distance tracking controller is used to ensure the safety of the intervehicle distance. The designed EACC system can realize the switching between the two controllers according to real-time information such as the relative distance between the main vehicle and the vehicle in front, so as to ensure driving safety. Owing to the complexity of intersection scenarios, planning speed is affected by many factors, such as signal duration, distance to the intersection, and initial planning speed. Hence, this paper further analyzes the sensitivity of the above factors to discuss their impact on EACC. In addition, in order to further improve the problem of low intersection traffic efficiency caused by only planning a single vehicle, this paper also provided an ACC fleet speed planning method based on V2X communication. Specifically, ACC vehicles can obtain the status of signal lights near intersections and the planned speed of vehicles in front and behind based on V2I and V2V communication. Then, these vehicles would form a fleet and plan the optimal speed sequence for each vehicle for tracking. When all vehicles in the fleet are traveling at the planned speed, the road capacity can be fully utilized, thereby improving the overall traffic efficiency of the intersection and reducing the average energy consumption of the fleet.

2 Modeling

In urban roads, ACC vehicles commonly pass through intersections. Although ACC vehicles can follow the vehicle immediately in front of them in the intersection, their performance is considerably influenced by the driving style of the vehicle in front of them. In scenarios in which V2X communication or computer vision exists, if ACC vehicles can obtain real-time signal status and its timings and use this information to plan the target speed, then the effect of the vehicle in front can be reduced and the ACC vehicle can pass the intersection at a flexible speed. Figure 1 reveals the schematic of the energy-optimized control system based on GA optimization at the intersection of intelligent connected electric vehicles. The modeling is explained below.

2.1 Scene definition

Because a vehicle passing through an intersection is highly complex, the passing behavior of the vehicle is related to the number of vehicles ahead and their driving status, the signal status and its timing, as well as the status of the host vehicle. Therefore, this study appropriately simplified assumptions to facilitate research. The following scenarios were defined for ACC vehicles through intersections.

(1) ACC vehicles passing the intersection under the scenario of no vehicle ahead.

(2) ACC vehicles pass the intersection when manually driven vehicles are ahead.

(3) Multi-vehicle intersection passing with internet connection status.

Vehicles in the three scenarios can obtain the signal light status information ahead and the number of vehicles ahead by V2X.

2.2 Vehicle longitudinal dynamics modeling

The vehicle longitudinal dynamics model depicts the relationship between the vehicle driving state and the control variable. Eq. (1) presents the transformation relationship between the motor torque and vehicle speed, and the driving state of the vehicle can be changed by controlling the torque of the motor when driving or braking.

$$m\frac{\mathrm{d}v}{\mathrm{d}t}=\frac{T_m i_t \eta}{r}-F_f-F_{\mathrm{air}}-F_i, \tag{1}$$

$$F_f=mgf\cos\alpha, \tag{2}$$

$$F_{\mathrm{air}}=\frac{C_w\rho A v^2}{2}, \tag{3}$$

$$F_i=mg\sin\alpha, \tag{4}$$

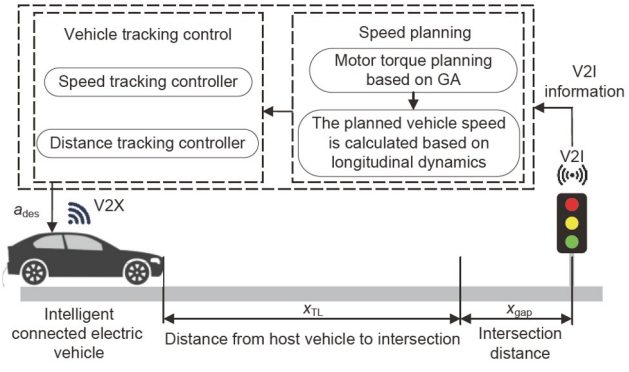

Figure 1 (Color online) Schematic of the energy-optimized control system at the intersection of intelligent connected electric vehicles based on GA optimization.

where m is the vehicle mass. v is the vehicle speed. T_m is the output torque of the motor. i_t is the product of the gear ratio deceleration device and the final reduction drive. η is the efficiency of the drive train. r is the wheel radius. F_f is the rolling resistance. F_{air} is the air resistance. F_i is the slope resistance. g is the acceleration of gravity, f is the rolling resistance coefficient, α is the road slope, C_w is the wind resistance coefficient, ρ is the air density, and A is the windward area. The calculation of rolling resistance, air resistance, and slope resistance is shown in eqs. (2)–(4).

Furthermore, the torque distribution strategy was adopted to divide the desired torque into the desired motor torque and desired hydraulic braking pressure. When the expected acceleration was less than zero, energy recovery was required according to the maximum braking torque that can be provided at the current vehicle speed, and the insufficient braking torque was compensated by hydraulic braking.

2.3 Motor energy consumption modeling

The vehicle longitudinal dynamics model reveals that the motor torque control can influence the driving state of the vehicle. Therefore, to reduce motor energy consumption, obtaining a suitable motor torque profile is essential so that the vehicle can drive at the optimal speed. The motor energy consumption characteristics determined from the experiments can be used to calculate the motor energy consumption corresponding to the motor output torque. Thus, the motor energy consumption can be included in the speed planning algorithm as an evaluation metric. The calculation of motor energy consumption is presented in eqs. (5) and (6). The working map of the motor obtained from the experiment is displayed in Figure 2.

$$P_m = \begin{cases} \dfrac{T_m n_m}{9550\eta_m}(T_m \geqslant 0), \\ \dfrac{T_m n_m}{9550}\eta_m(T_m < 0), \end{cases} \tag{5}$$

$$E_{\text{mot}} = \int_0^t P_m \mathrm{d}t, \tag{6}$$

where n_m is the motor speed. η_m is the motor efficiency. E_{mot} is the motor energy consumption. t is the integration duration variable. P_m is the motor power.

2.4 Vehicle traffic decision modeling

The ACC vehicle makes a passing behavior decision at the intersection when it obtains the real-time signal status, especially when the signal is green. Therefore, this study proposed a simple passing behavior decision method. As

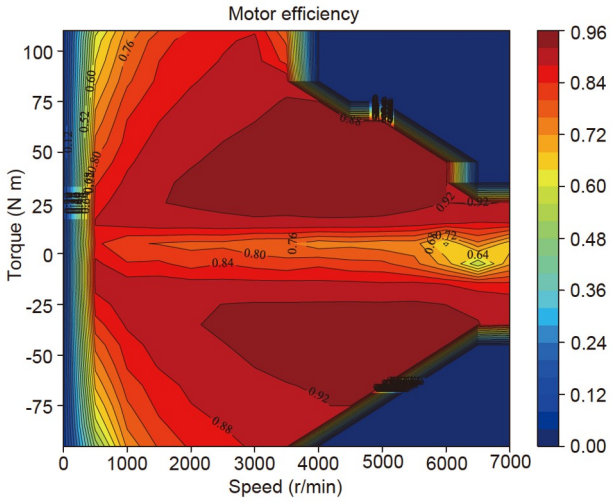

Figure 2 Motor working map.

presented in eq. (7), to obtain the passing decision, the average vehicle speed required for the vehicle to pass the intersection within the remaining green light duration is compared with the current vehicle speed. If the difference between the required average speed of the vehicle and the current speed is greater than 0, then the current vehicle cannot safely drive through the intersection in time with the average traffic flow speed within the effective remaining green light duration. At this stage, the passing decision Dec is equal to 0; otherwise it is equal to 1.

$$Dec = \begin{cases} 0, & \dfrac{x_{TL}+x_{\text{gap}}}{t_{\text{green\_left}}} - v_{\text{now}} > 0 \text{ or } TL = \text{red}, \\ 1, & \dfrac{x_{TL}+x_{\text{gap}}}{t_{\text{green\_left}}} - v_{\text{now}} \leqslant 0, \end{cases} \tag{7}$$

where x_{TL} is the distance of the vehicle from the intersection. x_{gap} is the length of the intersection. v_{now} is the current vehicle speed. $t_{\text{green\_left}}$ is the remaining green light duration. TL is the status of the signal light, which can be green, red or yellow.

2.5 Vehicle tracking modeling

Typically, the scenario of an ACC vehicle passing through an intersection is highly complex because timely intersection crossing under signal constraints as well as safety to avoid collision with other vehicles are necessary. When the ACC vehicle is in cruise mode, the vehicle simply tracks the desired vehicle speed output by the speed planning module. At this stage, the state variables of the controller are the difference between the actual speed and the expected velocity and host vehicle acceleration, and the control input is the expected acceleration. The tracking model is presented as follows:

$$\begin{bmatrix}\dot{v}_{\text{rel}}\\ \dot{a}_h\end{bmatrix}=\begin{bmatrix}0 & -1\\ 0 & -\frac{1}{\tau}\end{bmatrix}\begin{bmatrix}v_{\text{rel}}\\ a_h\end{bmatrix}+\begin{bmatrix}0\\ \frac{1}{\tau}\end{bmatrix}a_{\text{des}}+\begin{bmatrix}1\\ 0\end{bmatrix}a_{p1}, \tag{8}$$

where v_{rel} is the difference between the desired speed and the actual speed. a_h is the acceleration of the host vehicle. a_{des} is the desired acceleration. a_{p1} is the rate of change at the desired speed. When in cruise mode, the specific meaning is the rate of change of the planned speed obtained by the genetic algorithm (GA), and when it is in the following mode, the specific meaning is the rate of change of the speed of the preceding vehicle. Here τ is the hysteresis constant, and is used to simulate the delay caused by the response of sensors and actuators. An accurate hysteresis constant can effectively improve the effectiveness of the controller in transient and steady-state control.

When the workshop distance between the ACC vehicle and the front vehicle is less than the minimum safe workshop distance, the host vehicle should switch to the following mode to ensure the safe workshop distance. At this stage, the state variables of the controller are the relative distances between the host vehicle and the vehicle in front, the difference between the host vehicle speed and the front vehicle speed, and the host vehicle acceleration. Furthermore, the control input is the expected acceleration. The tracking model is as follows:

$$\begin{bmatrix}\dot{x}_{\text{rel}}\\ \dot{v}_{\text{rel}}\\ \dot{a}_h\end{bmatrix}=\begin{bmatrix}0 & 1 & -t_f\\ 0 & 0 & -1\\ 0 & 0 & -\frac{1}{\tau}\end{bmatrix}\begin{bmatrix}x_{\text{rel}}\\ v_{\text{rel}}\\ a_h\end{bmatrix}+\begin{bmatrix}0\\ 0\\ \frac{1}{\tau}\end{bmatrix}a_{\text{des}}+\begin{bmatrix}0\\ 1\\ 0\end{bmatrix}a_{p2}, \tag{9}$$

where t_f is the fixed headway. x_{rel} is the distance between the host vehicle and the preceding vehicle. a_{p2} is the acceleration of the preceding vehicle.

3 Speed planning and control

In urban traffic, ACC vehicles generally use the set cruise speed or the vehicle speed ahead as the target speed to track and follow. Although the ACC vehicle follows the preceding vehicle smoothly, the performance of the ACC vehicle is affected by the driving style of the vehicle driver in the front. Especially in intersection scenarios, the passing performance and economy of ACC vehicle is considerably influenced by the preceding vehicle's driving strategy through the intersection. This subsection proposed a speed planning method for intersection scenarios to reduce the effect of the preceding driving styles of the ACC vehicle and improve its performance through intersections as follows.

(1) Crossing intersections safely and quickly under the constraints of the signals.

(2) Reducing the probability of ACC vehicles stopping and waiting at red lights as well as the energy consumption caused by idling motors.

(3) Improving the economy of ACC vehicles through intersections by improving the operating point of motors.

3.1 Speed planning method

3.1.1 Rule-based speed planning method

To reduce the number of vehicle stops at intersections, the rule-based speed planning method can be used to solve the calculation for the target vehicle speed based on the law of uniform variable speed motion after obtaining real-time signal status, timing, and passing decision information. To compare the energy consumption corresponding to various speed curves, the vehicle should accelerate or decelerate again to the initial speed after passing the intersection. The speed planning method based on rules is described as follows: Rule 1 refers to the fact that the host vehicle first moved at a uniform variable speed motion and subsequently at a constant speed to pass the intersection. Finally, after crossing the intersection, a uniform variable speed motion is used to reach the initial speed. Rule 2 refers to the fact that the host vehicle crosses the intersection at a uniform variable motion within the traffic light duration, and subsequently reaches the initial speed at a uniform variable motion. The rule-based planning speed design is as follows:

$$v_{\text{rule}}=\begin{cases}v_{\text{init}}+at, & t<t_h,\\ v_{\text{init}}+at_h, & t_h\leqslant t\leqslant t_{\text{lim}},\\ v_{\text{init}}+at_h-\dfrac{a(t-t_{\text{lim}})}{(t_{\text{planning}}-t_{\text{lim}})}, & t_{\text{lim}}\leqslant t\leqslant t_{\text{planning}},\end{cases} \tag{10}$$

$$t_h=\begin{cases}\dfrac{(at_{\text{lim}}-\sqrt{(a^2t_{\text{lim}}{}^2+2a(v_{\text{init}}t_{\text{lim}}-x_{\text{constraint}}))})}{a}, & a<0,\\ \dfrac{(at_{\text{lim}}+\sqrt{(a^2t_{\text{lim}}{}^2+2a(v_{\text{init}}t_{\text{lim}}-x_{\text{constraint}}))})}{a}, & a\geqslant 0,\end{cases} \tag{11}$$

$$x_{\text{constraint}}=\begin{cases}x_{TL}+x_{\text{gap}}, & Dec=1,\\ x_{TL}, & Dec=0,\end{cases} \tag{12}$$

$$t_{\text{lim}}=\begin{cases}t_{\text{green\_left}}, & Dec=1,\\ t_{\text{green\_left}}+t_{\text{yellow}}+t_{\text{red}}, & TL=\text{green and } Dec=0,\\ t_{\text{red\_left}}, & TL=\text{red and } Dec=0,\end{cases} \tag{13}$$

where v_{rule} is the planning speed based on rules. v_{init} is the initial planning speed. t_h is the duration of uniformly variable speed motion, which is related to the desired acceleration. t_{lim} is the duration of signal restraint. $t_{\text{green\_left}}$ is the remaining green light duration. $t_{\text{red\_left}}$ is the remaining red-light duration. t_{yellow} is the maximum duration of the yellow light. t_{red} is the maximum duration of the red light. $x_{\text{constraint}}$ is the

intersection distance constraint. Here a is the desirable acceleration, and $a \in [a_{\min}, a_{\max}]$. Specifically, when $Dec = 1$, if $v_{\text{init}} t_{\text{green\_left}} > x_{TL} + x_{\text{gap}}$, then the vehicle can drive through the intersection with the current speed at a constant speed within the effective remaining green light duration, and the maximum and minimum accelerations are as follows: $a_{\max} = 0$, $a_{\min} = 2(x_{TL} + x_{\text{gap}} - v_{\text{init}} t_{\text{lim}}) / t_{\text{lim}}^2$. Otherwise, $a_{\max}$ is the maximum acceleration of the vehicle, and $a_{\min}$ does not change. If $Dec = 0$, then $a_{\max} = 2(x_{TL} - v_{\text{init}} t_{\text{lim}}) / t_{\text{lim}}^2$, and $a_{\min}$ is the maximum vehicle deceleration.

Although the rule-based speed planning method allows vehicles to cross the intersection with minimal stopping probability, the uniform speed strategy reduces planning flexibility. Moreover, the rule-based planning algorithm produces sudden speed changes during the transition between uniform and uniformly variable speeds, which is not conducive for improving vehicle comfort. The rule-based approach does not consider optimization from the perspective of motor energy consumption. The approach has some limitations in terms of improving the economy.

3.1.2 *Optimization-based planning method*

This study proposed an optimization-based approach to plan the vehicle speed. The model was solved by using motor torque as the optimization variable, motor energy consumption as the objective function, signal constraints, motor external characteristics, and intersection speed limit as constraints, to obtain the most economical motor torque sequence of ACC vehicle when passing through the intersection. Next, based on the vehicle system dynamics, the optimal speed sequence for planning can be obtained through calculation. The GA is an optimization algorithm based on natural selection and genetic mechanisms that can be used to iteratively update the optimized sequence, which increases the ability of global optimization. Therefore, the GA was to solve the constructed speed planning problem. Figure 3 displays the GA flowchart.

The use process of GA includes determining the fitness function and solving space, initializing the sequence and coding, selecting cross-mutations, and determining the iterative stopping conditions. The fitness function can use the objective function after linear or power scale transformation. The solution space refers to all feasible solutions that satisfy constraints and generally should consider equation constraints, inequality constraints, linear constraints, and nonlinear constraints. In case the fitness function of the GA is the motor energy consumption, the sequence to be optimized is the motor torque sequence within the speed planning time, and the optimization problem is presented in eq. (14). The signal light constraints $Cons_{TL}$ in intersection traffic scenarios are as follows:

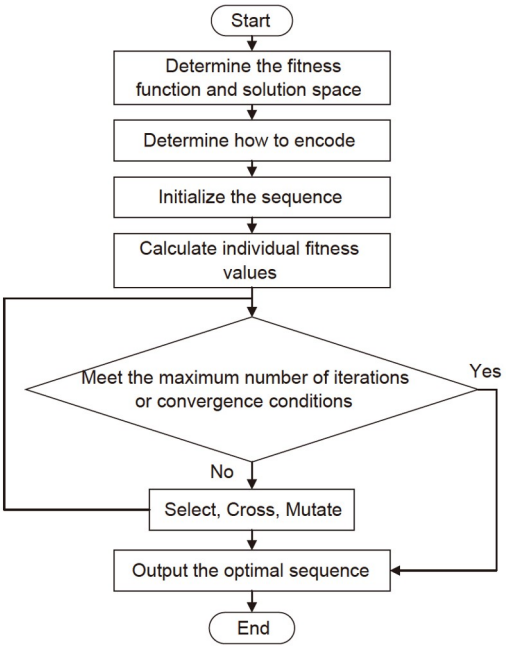

Figure 3 Genetic algorithm (GA) flowchart.

$$
\begin{aligned}
&T^* = \underset{T}{\operatorname{argmin}}\left(\sum_{i=1}^{N} T_m(i) n_m(i) \eta_m{}^{-\operatorname{sgn}(T_m(i))}\right),\\
&\text{s.t.}\quad m\frac{\mathrm{d}v}{\mathrm{d}t} = \frac{T_m i_t \eta}{r} - F_f - F_{\text{air}} - F_i,\\
&\qquad n_m = \frac{30 v i_t}{\pi r},\\
&\qquad \eta_m = f(T_m, n_m),\\
&\qquad (\Delta T_m)_{\min} < \Delta T_m < (\Delta T_m)_{\max},\\
&\qquad 0 \leqslant v(i) \leqslant v_{\text{lim}},\\
&\qquad a_{\text{lim1}} \leqslant a(i) \leqslant a_{\text{lim2}},\\
&\qquad Cons_{TL},
\end{aligned}
\tag{14}
$$

where T^* is the optimal torque sequence, that can be calculated to obtain the planning vehicle speed. The variation of motor efficiency with torque and speed can be acquired from the motor efficiency graph. Here ΔT_m is the variation of motor torque. $(\Delta T_m)_{\min}$ and $(\Delta T_m)_{\max}$ are the minimum and maximum magnitude of the motor torque variation, respectively. v_{lim} is the maximum speed limit at the intersection. Furthermore, a_{lim1}, a_{lim2} are the minimum and maximum constraints of vehicle acceleration, respectively. $Cons_{TL}$ is the signal constraints at intersections, defined differently in different scenarios, as shown in eqs. (15)–(17).

(1) When the signal is green and $Dec = 1$.

$$
Cons_{TL} = \begin{cases} \int_0^{t_{\text{planning}}} \int_0^{t_{\text{planning}}} \frac{1}{m}\left(\frac{T_m i_t \eta}{r} - F_f - F_{\text{air}} - F_i\right) \mathrm{d}t \mathrm{d}t > x_{TL} + x_{\text{gap}}, \\ v_{\text{end}} = v_{\text{init}}. \end{cases} \tag{15}
$$

(2) When the signal is green and $Dec = 0$.

$$Cons_{TL} = \begin{cases} \int_0^{t_{\text{planning}}} \int_0^{t_{\text{planning}}} \frac{1}{m}\left(\frac{T_m i_t \eta}{r} - F_f - F_{\text{air}} - F_i\right) \mathrm{d}t\mathrm{d}t > x_{TL} + x_{\text{gap}}, \\ \int_0^{t_{\text{lim}}} \int_0^{t_{\text{lim}}} \frac{1}{m}\left(\frac{T_m i_t \eta}{r} - F_f - F_{air} - F_i\right) \mathrm{d}t\mathrm{d}t > x_{TL} - n(L_1 + L_2) flag, \\ v_{\text{end}} = v_{\text{init}}. \end{cases} \tag{16}$$

(3) When the signal is red, we have the following:

$$Cons_{TL} = \begin{cases} \int_0^{t_{\text{lim}}} \int_0^{t_{\text{lim}}} \frac{1}{m}\left(\frac{T_m i_t \eta}{r} - F_f - F_{\text{air}} - F_i\right) \mathrm{d}t\mathrm{d}t < x_{TL} - n(L_1 + L_2) flag, \\ \int_0^{t_{\text{planning}}} \int_0^{t_{\text{planning}}} \frac{1}{m}\left(\frac{T_m i_t \eta}{r} - F_f - F_{\text{air}} - F_i\right) \mathrm{d}t\mathrm{d}t > x_{TL} + x_{\text{gap}}, \\ v_{\text{end}} = v_{\text{init}}, \end{cases} \tag{17}$$

where *flag* is the logical judgment, if there is a car ahead, its value is 1, otherwise it is 0. n is the number of preceding vehicles. v_{init} is the initial vehicle speed. v_{end} is the planning end speed. t_{lim} is the duration of the constraint, and t_{planning} is the planning duration.

Although the optimization of the speed trajectory from a single vehicle perspective in the described non-networked state can improve the driving economy and efficiency of the single vehicle, the planned speed may reduce the ride comfort or may even affect the average efficiency of the entire roadway because the method ignores the interaction between other traffic vehicles and this vehicle. In connected scenarios, because vehicles based on V2X communication can interact with other vehicles and road test units, forming a fleet and passing through intersections in time is easy. In this section, the centralized controller at the intersection is the object of study, and the vehicles that cross the intersection are queued according to the information on each vehicle's driving status at the intersection and the current signal status that is obtained by V2I. Therefore, the optimal speed sequence for each vehicle to track can be planned. Tables 1 and 2 present the two scenarios of a networked fleet speeding up through an intersection at a green light and slowing down through an intersection at a red light.

When the light is green, the centralized controller of the road test unit first determines whether each vehicle joins the fleet according to the passing policy in eq. (7), and only vehicles with a passing decision of 1 can form a fleet and drive through the intersection within the remaining green light duration. The serial number of the vehicle at the head of the fleet is 1, and the serial number of the vehicle at the tail is n. The objective function and constraint conditions of the problem to be optimized are the same as eq. (14), and next, the signal light constraint $Cons_{TLi}$ is designed. The centralized controller first performs speed planning for the vehicles at the rear of the queue, and its signal light constraint $Cons_{TLn}$ is presented in eq. (18). Thus, the planning speed should pass the intersection in time before the end of the green light. Next, based on the planned speed $g(T_i^*)$ of the vehicle i the centralized controller starts speed planning for the vehicle $i-1$. Vehicle $i-1$ signal light constraint $Cons_{TLi}$ is presents in eq. (19), which indicates planning vehicle speed $g(T_{i-1})$ should make the workshop distance between vehicle $i-1$ and vehicle i between the maximum desired workshop and the minimum desired workshop distances. According to the process, speed planning is performed for each vehicle in the fleet in turn, and the planned speed is sent to each vehicle based on V2I.

Table 1 Initial state of each networked vehicle accelerating to cross the intersection

Vehicle serial number	Initial distance from intersection (m)	Initial speed (m/s)
1	30	10
2	60	6
3	100	10
4	140	12
5	170	10
6	200	12

Table 2 Initial state of each networked vehicles decelerating to cross the intersection

Vehicle serial number	Initial distance from intersection (m)	Initial speed (m/s)
1	50	6
2	80	6
3	110	6
4	150	10
5	180	12

$$Cons_{TLn} = \int_0^{t_{\text{planning}}} \int_0^{t_{\text{planning}}} \frac{1}{m}\left(\frac{T_{\text{last}} i_t \eta}{r} - F_f - F_{\text{air}} - F_i\right) \mathrm{d}t\mathrm{d}t > x_{TL\_\text{last}} + x_{\text{gap}}, \tag{18}$$

$$x_{\text{des\_min}\_i} < Cons_{TLi} = \int_0^{t_{\text{planning}}} \left[g(T_{i-1}) - g(T_i^*)\right] \mathrm{d}t + x_{\text{init}\_i} < x_{\text{des\_max}\_i}, \tag{19}$$

where T_{last} is the torque sequence to be optimized for the rear vehicle n. x_{TL_last} is the distance from the trailing vehicle to

the intersection. $x_{\text{des\_min}\_i}$ is the minimum expected distance between vehicle i and vehicle $i-1$. $x_{\text{des\_max}\_i}$ is the maximum expected distance between vehicle i and vehicle $i-1$. x_{init_i} is the initial distance between vehicle i and vehicle $i-1$. The integrated object in eqs. (18) and (19) represent vehicle acceleration and velocity, respectively, so their integration times differ considerably.

When the light is red, the centralized controller first determines the length of the fleet, and then performs speed planning for lead vehicle 1. At this time, the signal constraint is presented in eq. (20), which reveals that the planning speed ensure its driving displacement does not cross the stop line before the end of the red light and drive through the intersection before the end of the green light. A margin d_0 should exist for other vehicles in the fleet to drive through the intersection in time. Next, based on the planned speed $g(T_i^*)$ of vehicle i, the centralized controller starts to plan the speed for vehicle $i+1$. The signal light constraint $Cons_{TLi}$ of vehicle $i+1$ is presented in eq. (21). Similarly, the planning speed $g(T_{i+1})$ should ensure the distance between vehicle $i+1$ and vehicle i between the maximum expected vehicle distance and the minimum expected vehicle distance. A margin d_i should exit to ensure that vehicles behind have sufficient space to drive through the intersection.

$$Cons_{TL1}=\begin{cases}\int_0^{t_{\text{lim}}}\int_0^{t_{\text{lim}}}\frac{1}{m}\left(\frac{T_0 i_t\eta}{r}-F_f-F_{\text{air}}-F_i\right)\mathrm{d}t\mathrm{d}t<x_{TL\_0},\\ \int_0^{t_{\text{planning}}}\int_0^{t_{\text{planning}}}\frac{1}{m}\left(\frac{T_0 i_t\eta}{r}-F_f-F_{\text{air}}-F_i\right)\mathrm{d}t\mathrm{d}t\\ \qquad >x_{TL\_0}+x_{\text{gap}}+d_0,\end{cases} \tag{20}$$

$$Cons_{TLn}=\begin{cases}x_{\text{des\_min}\_i+1}\leqslant\int_0^{t_{\text{planning}}}\left[g(T_{i+1})-g(T_i^*)\right]\mathrm{d}t\\ \qquad +x_{\text{init}\_i+1}<x_{\text{des\_max}\_i+1},\\ \int_0^{t_{\text{planning}}}\int_0^{t_{\text{planning}}}\frac{1}{m}\left(\frac{T_i i_t\eta}{r}-F_f-F_{\text{air}}-F_i\right)\mathrm{d}t\mathrm{d}t\\ \qquad >x_{TL\_i}+x_{\text{gap}}+d_i.\end{cases} \tag{21}$$

When the optimal motor torque sequence is obtained by the GA, the most economical planning speed for ACC vehicles through the intersection can be obtained through calculation. Because air resistance is positively correlated with vehicle speed, and the speed at the intersection is generally not too high due to the speed limit, this study ignored air resistance when planning the speed in the intersection scenario, that is, F_{air} is 0. The velocity planning time is t_{planning}, and discretization time interval be T_s. Therefore, the motor torque at the $n=t_{\text{planning}}/T_s$ time points should be optimized, the speed of the vehicle at the initial moment of planning is v_0. According to eq. (1), the vehicle speed at the first torque T_1 to be optimized is as follows:

$$v_1=v_0+\left(\frac{i_t\eta_t}{mr}T_1-gf\cos\alpha-g\sin\alpha\right)T_s. \tag{22}$$

Based on v_1, the speed at the second torque T_2 to be optimized can be calculated as follows:

$$v_2=v_0+\left(\frac{i_t\eta_t}{mr}T_1+\frac{i_t\eta_t}{mr}T_2-2(gf\cos\alpha+g\sin\alpha)\right)T_s. \tag{23}$$

For the same reason, the vehicle speed under other torques to be optimized T^* can be calculated, so the vehicle speed vector at each time can be expressed as follows:

$$\begin{bmatrix}v_1\\v_2\\\vdots\\v_n\end{bmatrix}=\begin{bmatrix}v_0\\v_0\\\vdots\\v_0\end{bmatrix}+\begin{bmatrix}\frac{i_t\eta_t}{mr}&0&\cdots&0\\\frac{i_t\eta_t}{mr}&\frac{i_t\eta_t}{mr}&\cdots&0\\\vdots&\vdots&\vdots&\vdots\\\frac{i_t\eta_t}{mr}&\frac{\eta_t}{mr}&\frac{i_t\eta_t}{mr}&\frac{i_t\eta_t}{mr}\end{bmatrix}_{n\times n}\begin{bmatrix}T_1\\T_2\\\vdots\\T_n\end{bmatrix}_{n\times n}T_s+\begin{bmatrix}-gf\cos\alpha-g\sin\alpha\\-2(gf\cos\alpha+g\sin\alpha)\\\vdots\\-n(gf\cos\alpha+g\sin\alpha)\end{bmatrix}_{n\times 1}T_s. \tag{24}$$

3.2 Intelligent driver model

To verify the effectiveness of the fleet speed planning method based on V2X communication, the energy consumption corresponding to the optimized vehicle speed is compared with the energy consumption under the IDM to verify the effectiveness of the connected fleet speed planning method in reducing the average energy consumption of the entire fleet. The established IDM is as follows:

$$s_{\text{ref1}}(v_h,\Delta v_1)=s_{\min}+v_h t_h+\frac{v_h\Delta v_1}{2\sqrt{a_{\max}a_c}}, \tag{25}$$

$$s_{\text{ref2}}(v_h,\Delta v_2)=s_{\min}+v_h t_h+\frac{v_h\Delta v_2}{2\sqrt{a_{\max}a_c}}, \tag{26}$$

$$a_{\text{des\_follow}}=a_{\max}\left[1-\left(\frac{v_h}{v_{\text{lim}}}\right)^{\delta}-\left(\frac{s_{\text{ref1}}(v_h,\Delta v_1)}{s_v}\right)^2\right], \tag{27}$$

$$a_{\text{des\_TL}}=a_{\max}\left[1-\left(\frac{v_h}{v_{\text{lim}}}\right)^{\delta}-\left(\frac{s_{ref2}(v_h,\Delta v_2)}{s_v+\text{gap}}\right)^2\right], \tag{28}$$

$$a_{\text{IDM1}}(s_c,v,\Delta v)=\begin{cases}a_{\text{des\_TL}}, & \text{if signal}(s_c)=0,\\ -\frac{{v_h}^2}{2{s_c}^2}, & \text{signal}(s_c)=1,\end{cases} \tag{29}$$

$$a_{\mathrm{IDM2}}(s_c, v, \Delta v) = \begin{cases} a_{\mathrm{des\_follow}}, & \mathrm{signal}(s_c)=0 \text{ and front}=0, \\ a_{\mathrm{des\_}TL}, & \mathrm{signal}(s_c)=0 \text{ and front}=1, \\ a_{\mathrm{des\_follow}}, & \mathrm{signal}(s_c)=1 \text{ and front}=0, \\ -\dfrac{{v_h}^2}{2{s_c}^2}, & \mathrm{signal}(s_c)=1 \text{ and front}=1, \end{cases} \tag{30}$$

where a_{IDM1} and a_{IDM2} are the expected acceleration of the fleet leader and other vehicles in the fleet, respectively. s_{ref1} is the desired vehicle spacing for the first vehicle in the fleet. s_{ref2} is the desired vehicle spacing for other vehicles in the fleet. Δv_1 is the difference between the vehicle at the head of the fleet and the speed limit on the road. Δv_2 is the relative speed between the other vehicles in the fleet and the vehicle in front. $s_{\min}$ is the minimum parking spacing. a_c is the comfortable deceleration value and is set to 1. Furthermore, δ is the relationship between the reduction of acceleration and the speed v_h. s_c is the distance between the host vehicle and the intersection. s_v is the distance between the host vehicle and the vehicle in front. signal(s_c) is the status of the traffic light at the current distance s_c, where 0 is green and 1 is red. front indicates whether the vehicle in front has currently driven through the intersection, where 0 indicates that it has not driven through the intersection, and 1 indicates that it has already driven through the intersection.

3.3 Controller design

The controller design of this study includes the speed-tracking and distance-tracking controllers. The speed-tracking controller is used to make the host vehicle track the planned speed, introduced in the last section. When the planned speed conflicts with the preceding vehicle speed, resulting in a sharp reduction of intervehicle distance, the distance controller intervenes to make the host vehicle track the desired intervehicle distance to ensure safety.

First, based on the exponential reaching law and variable speed reaching law, the sliding mode control (SMC) with compound reaching law was designed as the speed tracking controller. At this stage, the state variables of the controller are the difference between the actual speed and the expected velocity and the host vehicle acceleration, and the control input is the expected acceleration. Exponential reaching law and variable speed reaching law are as follows:

$$\dot{s} = -\varepsilon \cdot \mathrm{sgn}(s) - qs, \tag{31}$$

$$\dot{s} = -\varepsilon \|x\|_1 \mathrm{sgn}(s). \tag{32}$$

The sliding mode function is as follows:

$$s(k) = C_e(R(k) - x(k)). \tag{33}$$

According to eq. (33), the control law can be gained:

$$u(k) = (C_e B_1)^{-1}(C_e R(k+1) - C_e A_1 x(k) - s(k+1)). \tag{34}$$

When the exponential reaching law is selected, the sliding mode function in discrete state is as follows:

$$s(k+1) = T_s[-\varepsilon \cdot \mathrm{sgn}(s(k)) - qs(k)] + s(k). \tag{35}$$

When the variable speed reaching law is selected, the sliding mode function in discrete state is as follows:

$$s(k+1) = -T_s\varepsilon \|x(k)\|_1 \mathrm{sgn}(s(k)) + s(k). \tag{36}$$

Therefore, the desired acceleration output by the speed tracking controller based on the composite reaching law is as follows:

$$a_{\mathrm{des}}(k) = (C_e B_1)^{-1}(C_e R(k+1) - C_e A_1 x - s(k) - \mathrm{d}s(k)), \tag{37}$$

$$\mathrm{d}s(k) = \begin{cases} -\varepsilon T_s \mathrm{sgn}(s(k)) - qT_s s(k), & \mathrm{sat}(k) > sat_{\min}, \\ -\varepsilon T_s \mathrm{sgn}(s(k))\mathrm{sat}(k), & \mathrm{sat}(k) \leqslant sat_{\min}, \end{cases} \tag{38}$$

where $\mathrm{sat}(k) = \left|(v_{\mathrm{rel\_des}}(k) - v_{\mathrm{rel}}(k))\right| + \left|(a_{h\_\mathrm{des}}(k) - a_h(k))\right|$, $sat_{\min}$ is the threshold of reaching law switching.

Furthermore, the SMC based on linear matrix inequality is designed as the distance tracking controller. Here, $s = {B_2}^{\mathrm{T}}Px$ is the sliding mode function. The state variables of the controller are the relative distance between the host vehicle and the vehicle in front, the difference between the host vehicle speed and the front vehicle speed, and the host vehicle acceleration, and the control input is the expected acceleration. The equivalent control term and robust control term can be obtained from the equivalent control principle, as shown in eqs. (39) and (40).

$$u_{\mathrm{eq}} = -({B_2}^{\mathrm{T}}PB)^{-1}B^{\mathrm{T}}PA_2x(t), \tag{39}$$

$$u_n = -({B_2}^{\mathrm{T}}PB)^{-1}\left[|B^{\mathrm{T}}PB|\delta_f + \varepsilon_0\right]\mathrm{sgn}(s), \tag{40}$$

where δ_f is the upper bound of perturbation term, and $\varepsilon_0 > 0$. In order to make $u = u_{eq} + u_n$ meet the stability conditions, the matrix P is further designed. Rewrite the control law as $u = -Kx + v$, where $v = Kx + u_{eq} + u_n$. Lyapunov function is chosen as $v = x^{\mathrm{T}}Px$. By substituting the state equation and control law, it can be obtained as follows:

$$\begin{aligned} \dot{V} &= 2x^{\mathrm{T}}P\dot{x} = 2x^{\mathrm{T}}P\overline{A}x + 2x^{\mathrm{T}}PB_2v \\ &= x^{\mathrm{T}}(P\overline{A} + \overline{A}^{\mathrm{T}}P) + 2x^{\mathrm{T}}PB_2v, \end{aligned} \tag{41}$$

where $\overline{A} = A_2 - B_2K$. Due to u can make $s = {B_2}^{\mathrm{T}}Px = 0$, $\dot{V} < 0$ can be satisfied only by satisfying the following formula.

$$P\overline{A} + \overline{A}^{\mathrm{T}}P < 0. \tag{42}$$

Multiply both sides of the above formula by P^{-1} and make $X = P^{-1}$.

$$(A_2 - B_2K)X + X(A_2 - B_2K)^{\mathrm{T}} < 0, \tag{43}$$

Make $KX = L$ to linearization eq. (43).

$$A_2X - B_2L + Xc^{\mathrm{T}} - L^{\mathrm{T}}B_2{}^{\mathrm{T}} < 0, \tag{44}$$

where L and X can be calculated according to Matlab LMI toolbox. Then $P = X^{-1}$. Furthermore, the desired acceleration of the distance controller can be obtained by substituting P into the control law u.

$$a_{\mathrm{des}} = -\left(B_2{}^{\mathrm{T}}PB\right)^{-1}B^{\mathrm{T}}PA_2x(t) - \left(B_2{}^{\mathrm{T}}PB_2\right)^{-1}\left[|B^{\mathrm{T}}PB|\delta_f + \varepsilon_0\right]\mathrm{sgn}(s). \tag{45}$$

4 Simulation and performance comparison

In this section, the superiority of the proposed speed planning algorithm is verified by setting several specific scenarios, and the sensitivity analysis is performed on three factors, namely initial speed, remaining duration of traffic lights, and distance from the intersection, which influence speed planning at intersections. Finally, hardware-in-the-loop (HIL) tests were conducted to verify the effectiveness of the sliding mode controller under real-time conditions.

4.1 Simulation parameter design

In this study, an electric vehicle produced by an enterprise is used as the research object, and the motor used is a permanent magnet brushless DC motor. The relevant structural parameters and simulation parameter settings are presented in Table 3.

Table 3 Simulation parameter design

Parameter name	Value	Unit
Vehicle quality	775	kg
Rolling resistance coefficient	0.01117	–
Air resistance coefficient	0.25	–
Windward area	2.04	m^2
Gear ratio	6.515	–
Tire radius	0.252	m
Transmission efficiency	0.95	–
Fixed time headway	1	s
Minimum parking distance	5	m
Intersection distance (x_{gap})	20	m
Approaching velocity (ε)	4	–
Convergence coefficient (q)	4	–
upper bound of perturbation term (δ_f)	3	–
Initial approaching velocity (ε_0)	2	–
Maximum speed limit (v_{lim})	20	m/s
Minimum acceleration limit (a_{lim1})	−3	m/s^2
Maximum acceleration limit (a_{lim2})	2	m/s^2

Table 4 Traffic light status

Traffic light	Remaining duration	Unit
Red	20	s
Green	15	s
Yellow	3	s

4.2 Analysis of simulation results

4.2.1 Crossing the intersection when there is no vehicle is in front of the host vehicle

Scene definition: The host vehicle was driven at the speed of 12 m/s, 200 m away from the intersection and no vehicle was ahead. Table 4 presents the traffic light state information. The period of traffic light is 38 s including red light for 20 s, green light for 15 s, and yellow light for 3 s.

Case 1: The traffic light now is red, and the remaining time is 20 s. Therefore, the host vehicle should slow down to avoid stopping at the intersection. The rule-based speed planning method used to determine the vehicle's selectable deceleration was [−3,−0.2]. The speed corresponding to the two critical accelerations selected was the rule-based planning speed. The method of planning the vehicle speed with a critical acceleration of −0.2 m/s^2 is Rule 1, and the method of planning the vehicle speed with a critical acceleration of −3 m/s^2 is Rule 2. As in the displacement curve in Figure 4(a), when the host vehicle tracks the planned speed, it cannot exceed the stop line before the end of the red light and can pass the intersection smoothly at a green light. As displayed in the speed curve in Figure 4(b), both rule-based and optimization-based planning of the vehicle speed enables the host vehicle to maintain a certain speed through the intersection.

Case 2: The traffic light is green, and the remaining duration is 15 s. Therefore, the host vehicle should first accelerate to pass the intersection within the green light time. Based on the constraints of the signal length and the distance from the intersection and initial speed, the acceleration range of the vehicle was determined to be [0.35,2.0]. Similarly, the method of planning the vehicle speed with maximum acceleration to plan the speed was stipulated to be Rule 1, and the method of planning the vehicle speed with minimum acceleration to plan the speed was Rule 2. As displayed in Figure 4(c) and (d), both rule-based and optimization-based methods can pass intersections in time within the green light time when the host vehicle tracks the planned speed.

Table 5 presents the energy consumption performance of various speed planning methods in scenarios of Cases 1 and

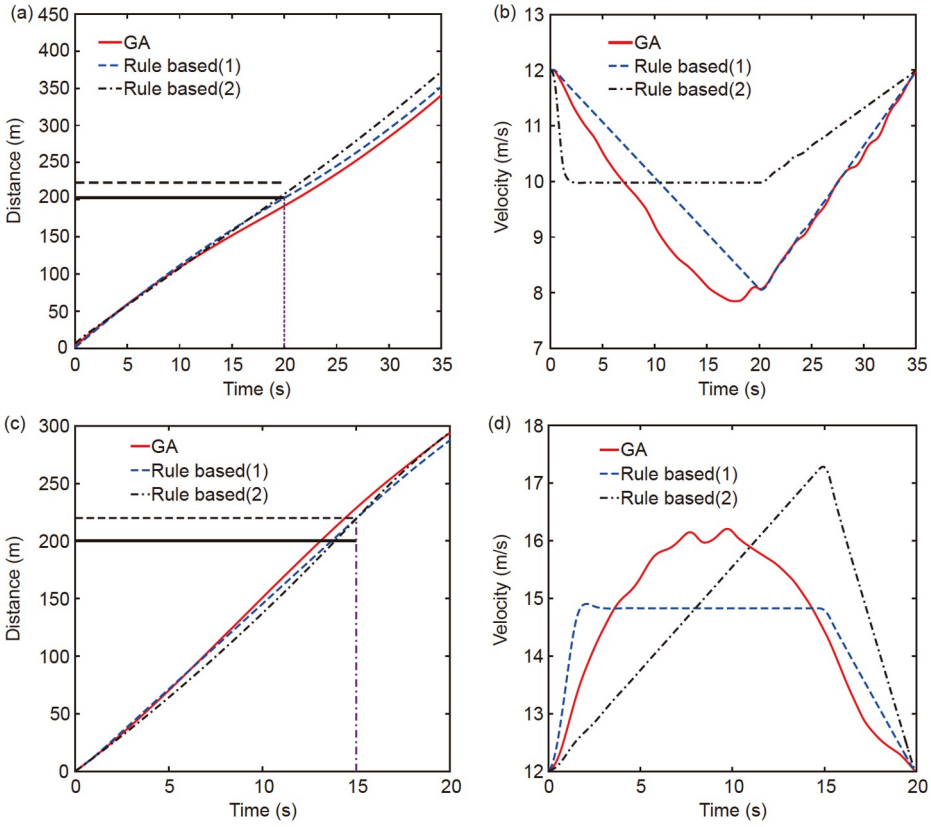

Figure 4 (Color online) Displacement and velocity curves of various speed planning methods in Cases 1 and 2. (a) Displacement curve of Case 1; (b) velocity curve of Case 1; (c) displacement curve of Case 2; (d) velocity curve of Case 2.

2. The table reveals that the method of GA in Case 1 is close to the energy consumption of Rule 1, but is more energy efficient compared with the method of Rule 2. Figure 4(a) and (b) and Figure 5(a) reveal that the primary cause of the similarity in energy consumption between the GA method and the Rule 1 method is the planning speeds of the two methods are similar and the torque performance is similar. Therefore, the difference in energy consumption between the two is not obvious. Compared with the Rule 2 method, the torque diagram of Figure 5(a) reveals that the primary reason for the lower energy consumption of the GA method is that it avoids the emergency braking caused by sharp deceleration, which reduces the energy lost to overcome hydraulic braking resistance. In Case 2, Table 5 reveals that the GA method resulted in a considerable reduction in energy consumption and improved fuel economy by nearly 16% compared with that in the Rule 2-based method. The torque diagram of Figure 5(b) reveals that the primary reason for the reduction of energy consumption compared with the planning speed of Rule 1 is that the GA method reduces the peak torque output of the motor, which reduces the high power consumption caused by the peak torque. Compared with the Rule 2 method, the primary reason for the reduction of energy

Table 5 Energy consumption comparison of Cases 1 and 2

Example scenario	GA	Rule 1	Rule 2	Unit
Case 1	0.0309	0.0305	0.0341	kW h/km
Case 2	0.0426	0.0455	0.0510	kW h/km

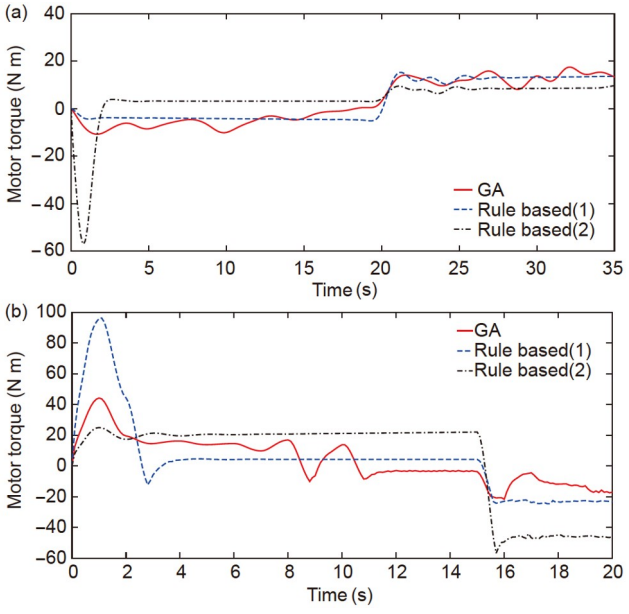

Figure 5 (Color online) The motor torque using different planning methods. (a) Case 1; (b) Case 2.

consumption of the GA method is that it has a shorter time to maintain the positive torque output, and the braking torque required when braking is small. Therefore, the hydraulic brake compensation is less, the energy recovery efficiency is higher, and the energy consumption performance is better.

4.2.2 Crossing the intersection when vehicles are in front of the host vehicle

Scene definition: Two manual vehicles are going through the intersection in front of the host vehicle. For the red light, because human drivers generally slow down and wait for the traffic light to turn green, modifying the displacement constraints when planning the speed is critical to avoid a collision between the host vehicle and the front vehicle.

Case 3: The host vehicle is driving at a speed of 10 m/s and is 200 m away from the intersection. At this time, the traffic light is red, and the remaining time is 15 s. Two manual vehicles ahead are about to cross the intersection. As displayed in Figure 6(a) and (b), when the host vehicle tracks the planned speed, the vehicle can ensure a safe distance from the vehicle in front of it, decelerate to a speed of 1 m/s before the traffic light turns green to avoid collision, and can pass the intersection in time after the light turns green. However, the simulation reveals that the vehicle-to-vehicle distance between the host vehicle and the vehicle in front is large at some time, and it crosses the intersection in the last second of the green light. Although these behaviors could make the host vehicle perform economically, from the perspective of the whole traffic flow, it reduces road traffic efficiency and increases the average travel time. Therefore, only considering the optimization of a single vehicle is not necessarily conducive to improving road traffic efficiency.

Case 4: The host vehicle is driving at a speed of 12 m/s and is 200 m away from the intersection. The traffic light is green, and the remaining time is 5 s. Two manual vehicles ahead are about to cross the intersection. Therefore, the planned speed should ensure the host vehicle does not exceed the stop line before the next green light starts. As displayed in the displacement curve in Figure 6(c), the host vehicle can maintain a safe vehicle-to-vehicle distance from the vehicle in front and pass the intersection in time for the next green light. As depicted in the curve of vehicle-to-vehicle distance between the host vehicle and the preceding one in Figure 6(d), the distance reaches the preset threshold of 25 m at 13.6 s. If the controlled vehicle continues to track the planned speed, it may collide because the distance between vehicles is too small. Therefore, the speed controller is switched to the distance controller at this time, and the distance between vehicles starts to track the expected distance between vehicles determined by the constant headway.

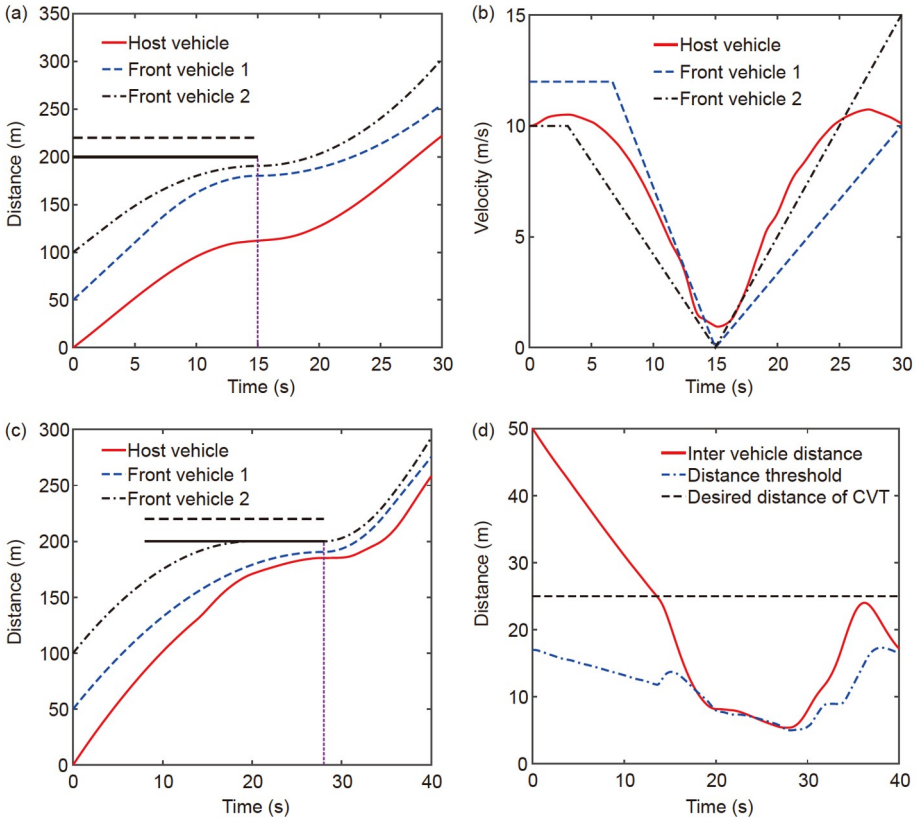

Figure 6 (Color online) Displacement and velocity curves in the scenario of vehicles ahead. (a) Displacement curve of Case 3; (b) velocity curve of Case 3; (c) displacement curve of Case 4; (d) intervehicle distance curve of Case 4.

4.2.3 *Sensitivity analysis*

The analysis revealed that factors affecting the performance of the planned speed include the initial speed, traffic light status, and its timing as well as the distance to the intersection. The analysis only verifies the superiority of the speed planning method based on the optimization and the effectiveness of the designed controller in some specific scenarios. The sensitivity of these factors affecting the speed optimization was analyzed to provide guidance for energy optimization speed planning at intersections.

(1) Sensitivity of the initial speed

The host vehicle is 200 m away from the intersection, and the current traffic light is green with 15 s remaining. The traffic decision is 1, which reveals that the host vehicle should pass through the intersection within 15 s. The energy consumption curve under various initial planning speeds is presented in Figure 7(a). When the initial planning speed is in the range of 12.5 to 15 m/s, the energy consumption per kilometer is the lowest. As displayed in Figure 8(a) and (b), when the planning speed is 12.5 to 15 m/s, the host vehicle can maintain a stable speed through the intersection.

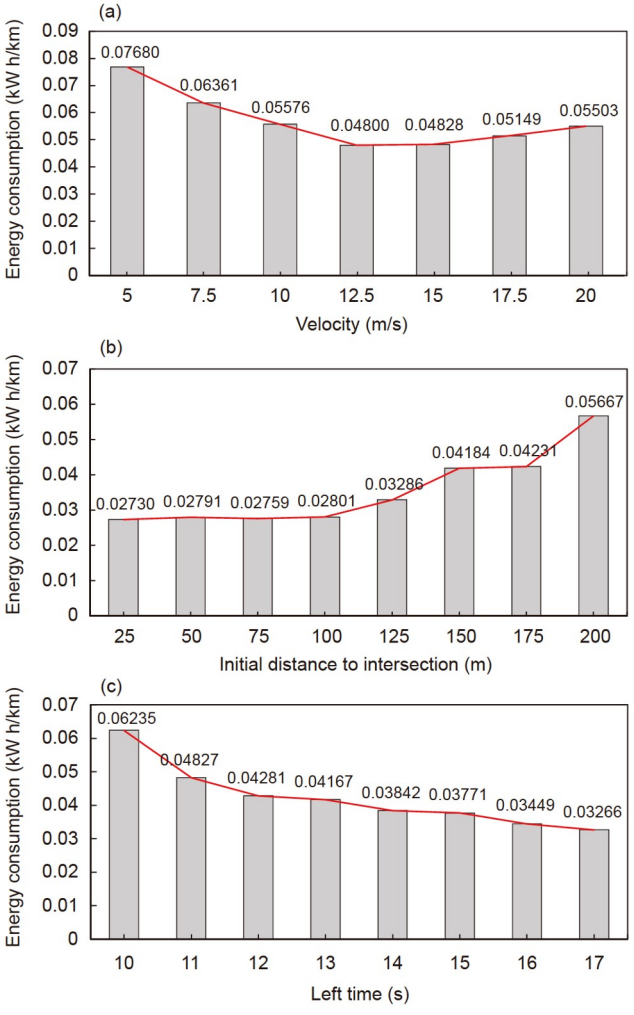

Figure 7 (Color online) Energy consumption performance under various influencing factors. (a) Initial speed sensitivity; (b) initial distance to intersection sensitivity; (c) remain traffic light duration sensitivity.

(2) Sensitivity of the distance to the intersection

The host vehicle drives at the intersection at the speed of 10 m/s, and the current traffic light is green with 15 s remaining. The traffic decision is 1, which reveals that the host vehicle should pass through the intersection within 15 s. The curve of energy consumption under various distances to the intersection is displayed in Figure 7(b). When the distance is less than 100 m, the energy consumption of the planned speed is positive and energy consumption between various distances does not differ considerably. However, when the distance exceeds 100 m, the energy consumption increases considerably. As displayed in Figure 8(c) and (d), when the distance between the host vehicle and the intersection is less than 100 m, the host vehicle can pass the intersection at an average speed or with appropriate deceleration, whereas when the distance is more than 100 m, the vehicle should accelerate through the intersection within the time of green light. Therefore, vehicle speed planning in advance based on V2X information can reduce the probability of vehicle idling at the red light and improve vehicle economy and traffic efficiency.

(3) Sensitivity of remain traffic light duration

The host vehicle travels at the speed of 12 m/s, 150 m away from the intersection and the traffic light is green. The traffic decision is 1, which reveals that it should pass through the intersection within the time of the green light. The remaining green light time is set from 10 to 17 s. As displayed in Figure 7(c), with the remaining green light duration increases, the energy consumption decreases. Figure 8(e) and (f) reveal that the trend of the planned speed gradually changes from first accelerating and subsequently decelerating to decelerating first and subsequently accelerating. This result is consistent with the sensitivity analysis of the other two factors. Thus, keeping the host vehicle driving at a stable speed to cross the intersection is conducive to reducing its energy consumption.

4.2.4 *Speed planning for the vehicle fleet with networking*

In Parts A and B, the speed trajectory is optimized from the perspective of the optimal economic performance of a single vehicle to improve the driving performance in various scenarios. The results revealed that although the economic performance of the single vehicle improved, the planning speed may cause excessive distance between the host vehicle and the vehicle in front, which reduces the efficiency of intersection traffic and increases the average energy consumption of the fleet. Therefore, the speed planning method of the GA fleet based on V2X communication should be studied further to coordinate and control each vehicle from the perspective of the vehicle platoon.

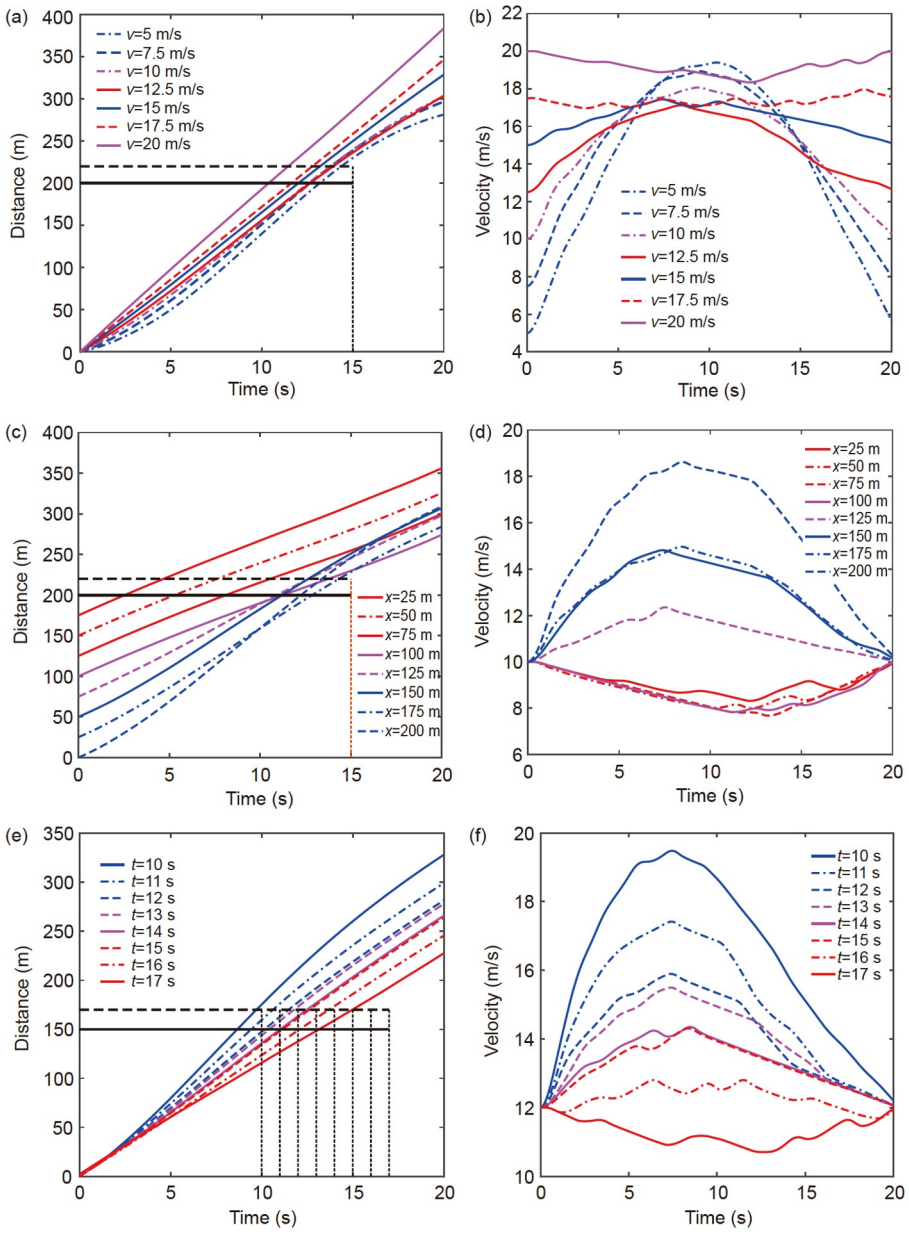

Figure 8 Displacement and velocity curves under various sensitivity factors. (a) Displacement of initial speed sensitivity; (b) velocity of initial speed sensitivity; (c) displacement of initial distance to intersection sensitivity; (d) velocity of initial distance to intersection sensitivity; (e) displacement of remain traffic light duration sensitivity; (f) velocity of remain traffic light duration sensitivity.

Case 5: The traffic light is green, and the remaining time is 15 s. As displayed in the displacement curve in Figure 9(a), when taking the speed planning method for the GA fleet, six vehicles at various distances from the intersection can form a vehicle platoon and pass the intersection in time. The inter-vehicle distance between each vehicle is small but safe. Therefore, more vehicles can cross the intersection at a time. As displayed in the speed curve in Figure 9(b), each vehicle in the fleet composed of six vehicles can accelerate appropriately through the intersection in time and can eventually tend to traverse at the same speed to realize smooth following.

Case 6: The traffic light is red, and the remaining time is 15 s. The simulation result under the red light is displayed in Figure 9(c) and (d). All vehicles in the fleet can decelerate appropriately at the end of the red light to ensure that they do not cross the stop line and maintain a safe intervehicle distance, and after the green light starts, they can accelerate to go through the intersection in time. Similarly, the final speed of the fleet tends to be the speed of the first vehicle in the platoon.

To illustrate the effectiveness of the GA fleet planning method based on V2X communication, this study compared the energy consumption of the GA fleet with the energy

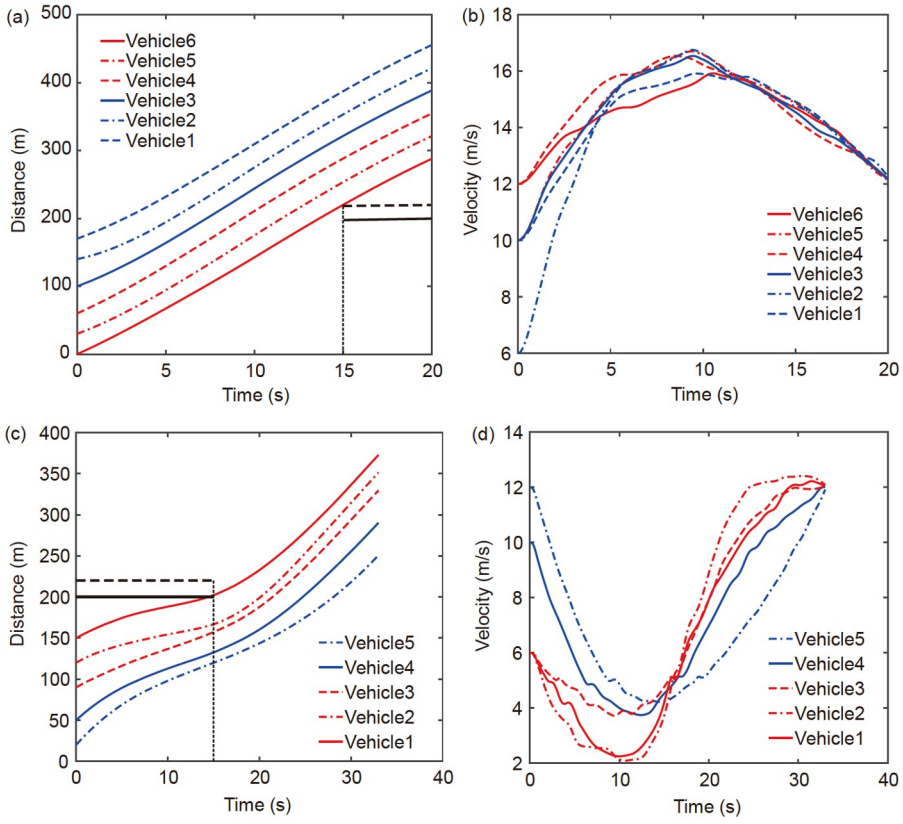

Figure 9 Displacement and velocity curves of connected fleet using the GA planning method. (a) Displacement curve of Case 5; (b) velocity curve of Case 5; (c) displacement curve of Case 6; (d) velocity curve of Case 6.

consumption of the IDM fleet [6] and the ACC fleet [29]. Figure 10(a) and (b) displays the displacement curve of the IDM fleet in Cases 5 and 6. Figure 10(c) and (d) displays the displacement curve of the ACC fleet that only plans the speed of the front vehicle in Cases 5 and 6 scenarios. In the green light acceleration through the intersection scenario, as shown in Figure 10(a), because the last vehicle of the IDM model fleet could not pass the intersection during the remaining green light time, the high-power consumption when stationary increased, which extended the average travel time. Figure 10(c) reveals that similar to the IDM the ACC fleet should maintain a large safety car spacing, resulting in the last vehicle not being able to accelerate through the intersection in time for the remaining green light time, the high-power consumption during stationary increases and extends the average travel time. In the red-light deceleration scenario through the intersection, as displayed in Figure 10(b), because the first vehicle of the IDM fleet cannot pass the intersection in time, all vehicles in the fleet should stop and wait for the red light before passing, which considerably increases high power consumption when the fleet is stationary and starting. As displayed in Figure 10(d), because of the speed planning of the first vehicle, although the ACC fleet can ensure that all vehicles can pass through the intersection without stopping, the following speed of the rear car is always affected by the speed of the vehicle in front. Therefore, optimal energy consumption cannot be guaranteed. The average energy consumption performance of the fleet through the intersection using different fleet speed planning methods is presented in Table 6. The results revealed that using motor energy consumption as a cost function of the connected fleet speed planning algorithm can plan a suitable speed curve for each vehicle to maintain a small safe distance, which improves traffic efficiency and reduces average fleet energy consumption. The results revealed that the GA fleet planning method based on network connection reduced the average fleet energy consumption by 26% compared with the IDM-based method in the green light acceleration scenario. Compared with the ACC fleet, which only plans the speed of the vehicle in front, the average fleet energy consumption is reduced by 24%. In the red-light scenario, the GA fleet planning method based on network connection reduces the average fleet energy consumption by 15% compared with the IDM-based method, and the average energy consumption is reduced by 7.6% compared with the ACC fleet that only plans the speed of the vehicle in the front.

4.2.5 Hard-ware in the loop

To evaluate the response characteristics of the proposed controller and verify its effectiveness under real-time con-

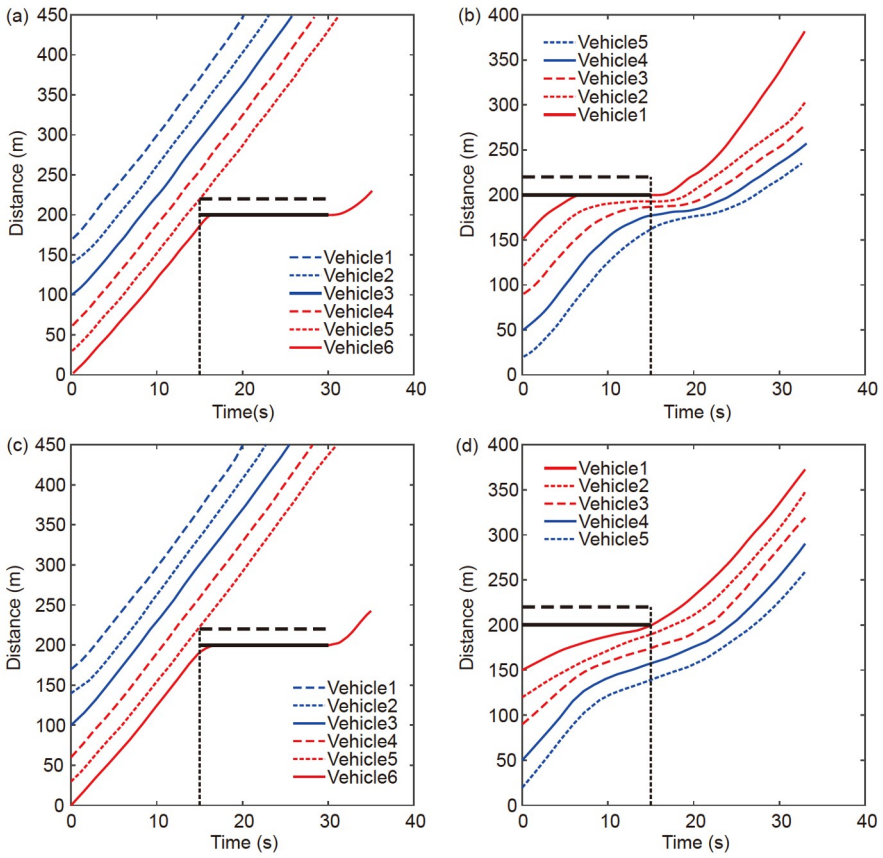

Figure 10 Displacement curve of the IDM and ACC fleet crossing the intersection. (a) Displacement of the IDM fleet under Case 5; (b) displacement of the IDM fleet under Case 6; (c) displacement of the ACC fleet under Case 5; (d) displacement of the ACC fleet under Case 6.

Table 6 Comparison of average energy consumption of the fleet crossing the intersection

Method	The green light accelerates through the intersection	The red light decelerates through the intersection	Unit
GA energy consumption	0.0679	0.0816	kW h/km
IDM energy consumption	0.0918	0.0961	kW h/km
ACC energy consumption	0.0895	0.0883	kW h/km

ditions, the HIL test was performed to consider communication and computing resource allocation in practice. The platform developed for HIL includes ECU rapid prototype development based on D2P and simulation model construction based on the NI real-time simulator provided by the test cabinet. As presented in Figure 11, MotoHawk was used to develop the proposed controller, which was subsequently converted to the C code and written into the ECU. The selected ECU was ECU-565-128, and Motorola MPC565 was used as the processor. NI PXIe-8135 supplied by the HCU HIL system was used as the processor of NI real-time simulator. CAN communication between ECU and test cabinet was performed according to the configured DBC file for exchanging information. Because offline optimization and online control were used, the real-time nature of GA is not involved when performing HIL experiments and is only used to verify the effectiveness and real-time performance of the controller. Figure 12 displays the experimental results obtained from the human-machine interface software. Compared with the results of the simulation shown in Figure 6(c) and (d), the result of HIL in Figure 12(a) and (b) reveals that the distance tracking controller and speed tracking controller can be switched smoothly according to the real-time driving environment under real-time conditions. Compared with the results of the simulation in Figure 9 detailing the scenario of crossing the intersection with vehicle fleet speed planning, the results of HIL in Figure 12(c) and (d) reveal that although a certain fluctuation occurs in the vehicle speed, the proposed speed tracking controller can make each vehicle keep the safe intervehicle distance from the vehicle in front or behind and cross the intersection in time.

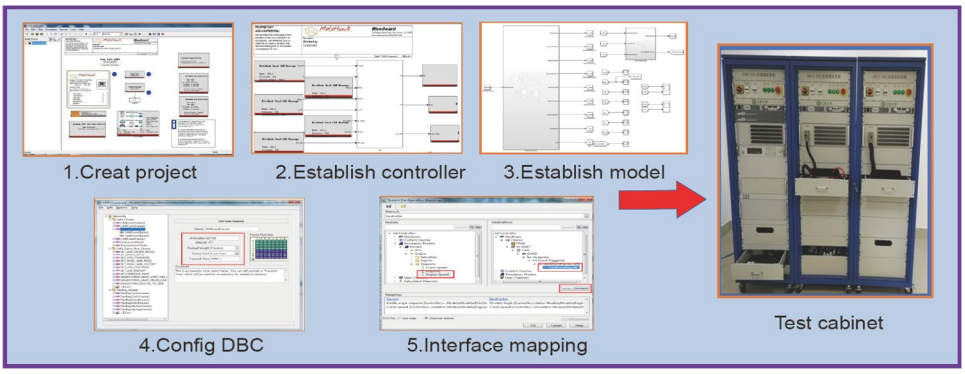

Figure 11 Hardware-in-loop (HIL) platform.

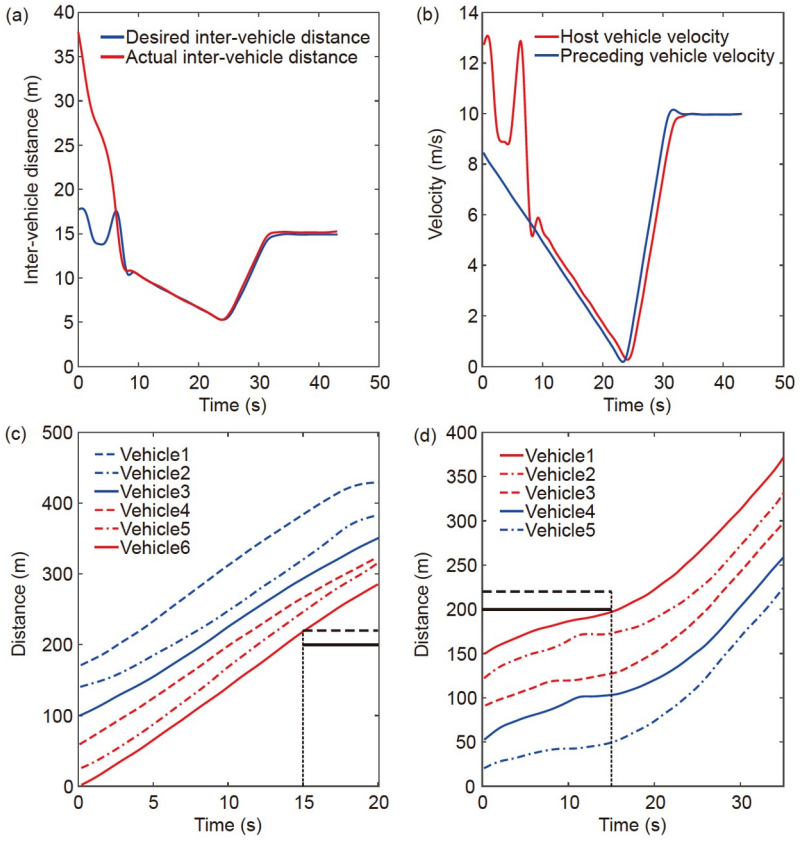

Figure 12 HIL results. (a) HIL displacement tracking curve of slowing down to cross the intersection at the red light. (b) HIL speed tracking curve of slowing down to cross the intersection at the red light. (c) HIL displacement curve under Case 5. (d) HIL displacement curve under Case 6.

5 Conclusions

In this study, the EACC design under the intersection scenario was investigated. By introducing speed planning, an ACC vehicle can safely cross the intersection at an economical speed to satisfy traffic light constraints. The simulation results under various scenarios revealed that although the tracking of the planned speed can reduce the effect of the driving style of the front vehicle on the host vehicle to obtain the local optimal economic performance, the intervehicle distance may be too large or small and time required to cross the intersection may be too large and too switched between speed controller and distance controller. Therefore, this study proposed a speed planning method for vehicle platoons based on V2X communication. By planning the speed of each vehicle in the fleet according to a certain order and considering the intervehicle distance as the constraint, efficient coordinated control of the vehicles in the fleet can be achieved. The simulation results revealed that vehicles can travel in a platoon with smaller and safer vehicle spacing,

which can improve road traffic efficiency and the average energy consumption of the fleet. The conclusions of this study are as follows.

(1) The speed planning method comparison between rule-based and GA-based revealed that the GA-based method can obtain superior energy consumption performance because the motor energy consumption is considered as the loss function, which can reduce the output motor torque peak and maintain a stable torque output.

(2) Based on V2X communication, the GA speed planning for each vehicle from the perspective of the vehicle platoon can obtain the global optimal speed profile. The flexible and variable vehicle intervehicle distance enables more vehicles to pass through the intersection in time to improve the traffic efficiency of the road and the average energy consumption of the fleet.

(3) Sensitivity analysis of the initial speed, the remaining traffic light duration, and the distance to the intersection reveals that the optimal economic performance can be obtained when the vehicle can maintain a uniform speed to cross the intersection. A large acceleration and deceleration could reduce the economic performance of the vehicle.

Effectively modeling the decision-making behavior of joining or leaving a fleet and planning vehicle speeds in a V2X environment under mixed traffic flows are critical topics of research in the future.

This work was supported by the National Natural Science Foundation of China (Grant No. 52272367).

1 Feng Y, Yu C, Liu H X. Spatiotemporal intersection control in a connected and automated vehicle environment. Transp Res Part C, 2018, 89: 364–383
2 Pan C, Huang A, Chen L, et al. A review of the development trend of adaptive cruise control for ecological driving. Proc Instit Mech Eng Part D, 2022, 236: 1931–1948
3 Wang Q, Ju F, Zhuang W C, et al. Ecological cruising control of connected electric vehicle: A deep reinforcement learning approach. Sci China Tech Sci, 2022, 65: 529–540
4 Liu H, Wei H, Zuo T, et al. Fine-tuning ADAS algorithm parameters for optimizing traffic safety and mobility in connected vehicle environment. Transp Res Part C, 2017, 76: 132–149
5 Sun W, Zheng J, Liu H X. A capacity maximization scheme for intersection management with automated vehicles. Transp Res Part C-Emerging Technologies, 2018, 94: 19–31
6 Ma F, Yang Y, Wang J, et al. Eco-driving-based cooperative adaptive cruise control of connected vehicles platoon at signalized intersections. Transp Res Part D, 2021, 92: 102746
7 Vajedi M, Azad N L. Ecological adaptive cruise controller for plug-in hybrid electric vehicles using nonlinear model predictive control. IEEE Trans Intell Transp Syst, 2016, 17: 113–122
8 Zhou Y Z, Wang R C, Ding R K, et al. Investigation on hierarchical control for driving stability and safety of intelligent HEV during car-following and lane-change process. Sci China Tech Sci, 2021, 65: 53–76
9 Gao Z, LaClair T, Ou S, et al. Evaluation of electric vehicle component performance over eco-driving cycles. Energy, 2019, 172: 823–839
10 He X, Wu X. Eco-driving advisory strategies for a platoon of mixed gasoline and electric vehicles in a connected vehicle system. Transp Res Part D, 2018, 63: 907–922
11 HomChaudhuri B, Vahidi A, Pisu P. Fast model predictive control-based fuel efficient control strategy for a group of connected vehicles in urban road conditions. IEEE Trans Contr Syst Technol, 2017, 25: 760–767
12 Yang Y, Ma F, Wang J, et al. Cooperative ecological cruising using hierarchical control strategy with optimal sustainable performance for connected automated vehicles on varying road conditions. J Cleaner Prod, 2020, 275: 123056
13 Pan C, Huang A, Wang J, et al. Energy-optimal adaptive cruise control strategy for electric vehicles based on model predictive control. Energy, 2022, 241: 122793
14 Liu H, Lu X Y, Shladover S E. Traffic signal control by leveraging cooperative adaptive cruise control (CACC) vehicle platooning capabilities. Transp Res Part C, 2019, 104: 390–407
15 Xu B, Ban X J, Bian Y, et al. Cooperative method of traffic signal optimization and speed control of connected vehicles at isolated intersections. IEEE Trans Intell Transp Syst, 2019, 20: 1390–1403
16 Silgu M A, Erdağı İ G, Çelikoğlu H B. Network-wide emission effects of cooperative adaptive cruise control with signal control at intersections. Transp Res Procedia, 2020, 47: 545–552
17 Zhao J, Li W, Wang J, et al. Dynamic traffic signal timing optimization strategy incorporating various vehicle fuel consumption characteristics. IEEE Trans Veh Technol, 2016, 65: 3874–3887
18 Aziz H M A, Zhu F, Ukkusuri S V. Learning-based traffic signal control algorithms with neighborhood information sharing: An application for sustainable mobility. J Intel Transp Syst, 2018, 22: 40–52
19 Mandava S, Boriboonsomsin K, Barth M. Arterial velocity planning based on traffic signal information under light traffic conditions. In: The 12th International IEEE Conference on Intelligent Transportation Systems. St. Louis, 2009. 1–6
20 Jiang H, Hu J, An S, et al. Eco approaching at an isolated signalized intersection under partially connected and automated vehicles environment. Transp Res Part C, 2017, 79: 290–307
21 Kamalanathsharma R K, Rakha H A. Multi-stage dynamic programming algorithm for eco-speed control at traffic signalized intersections. In: 16th International IEEE Conference on Intelligent Transportation Systems. The Hague, 2013. 2094–2099
22 Lin Q, Li S E, Xu S, et al. Eco-driving operation of connected vehicle with V2I communication among multiple signalized intersections. IEEE Intell Transp Syst Mag, 2021, 13: 107–119
23 Tang X, Duan Z, Hu X, et al. Improving ride comfort and fuel economy of connected hybrid electric vehicles based on traffic signals and real road information. IEEE Trans Veh Technol, 2021, 70: 3101–3112
24 Liu B, Sun C, Wang B, et al. Adaptive speed planning of connected and automated vehicles using multi-light trained deep reinforcement learning. IEEE Trans Veh Technol, 2022, 71: 3533–3546
25 Lu Y, Xu X, Ding C, et al. A speed control method at successive signalized intersections under connected vehicles environment. IEEE Intell Transp Syst Mag, 2019, 11: 117–128
26 Chen Q, Zhao W, Li L, et al. ES-DQN: A learning method for vehicle intelligent speed control strategy under uncertain cut-in scenario. IEEE Trans Veh Technol, 2022, 71: 2472–2484
27 Li L, Zhao W, Wang C. POMDP motion planning algorithm based on multi-modal driving intention. IEEE Trans Intell Veh, 2023, 8: 1777–1786
28 Li L, Zhao W, Wang C, et al. BRAM-ED: Vehicle trajectory prediction considering the change of driving behavior. IEEE ASME Trans Mechatron, 2022, 27: 5690–5700
29 Lazar C, Tiganasu A, Caruntu C F. Arterial intersection improvement by using vehicle platooning and coordinated start. IFAC-PapersOnLine, 2018, 51: 136–141